








Letter

Evidence for Alfvén eigenmodes driven by alpha particles in D-³He fusion experiments on JET

V.G. Kiptily^{1,a,*} , M. Fitzgerald¹, Ye.O. Kazakov² , J. Ongena² ,
M. Nocente^{3,4} , S.E. Sharapov¹ , M. Dreval^{5,6} , Ž. Štancar⁷,
T. Craciunescu⁸, J. Garcia⁹ , L. Giacomelli⁴, V. Goloborodko¹⁰,
H.J.C. Oliver¹, H. Weisen¹¹ and JET Contributors^a

¹ United Kingdom Atomic Energy Authority, Culham Centre for Fusion Energy, Culham Science Centre, Abingdon, Oxon, OX14 3DB, United Kingdom of Great Britain and Northern Ireland

² Laboratory for Plasma Physics, LPP-ERM/KMS, TEC Partner, Brussels, Belgium

³ Dipartimento di Fisica, Università di Milano-Bicocca, Milan, Italy

⁴ Institute for Plasma Science and Technology, National Research Council, Milan, Italy

⁵ Institute of Plasma Physics, National Science Center Kharkov Institute of Physics and Technology, Kharkov 61108, Ukraine

⁶ V.N. Karazin Kharkiv National University, Kharkiv, Ukraine

⁷ Jožef Stefan Institute, Ljubljana, Slovenia

⁸ National Institute for Laser, Plasma and Radiation Physics, Bucharest, Romania

⁹ CEA, IRFM, Saint-Paul-lez-Durance, France

¹⁰ Institute for Nuclear Research, Kyiv, Ukraine

¹¹ Ecole Polytechnique Fédérale de Lausanne (EPFL), Swiss Plasma Center (SPC), Lausanne, Switzerland

E-mail: Vasili.Kiptily@ukaea.uk

Received 28 June 2021, revised 19 August 2021

Accepted for publication 14 September 2021

Published 12 October 2021



CrossMark

Abstract

Alfvén eigenmodes (AEs) driven by energetic alpha particles can lead to enhanced fast ion transport and losses, thereby degrading the plasma performance in ITER and future magnetic confinement fusion reactors. Unexpectedly, AEs with negative toroidal mode numbers, which are currently not considered for ITER, were observed in dedicated experiments with fusion-born alpha particles on the tokamak Joint European Torus (JET). The paper provides evidence for a complex interplay between fast ions, monster sawtooth crashes and AEs. Our results highlight the need for an improved description of the synergies between different fast ion phenomena in future burning plasmas.

Keywords: tokamak, fast-ions, fusion-born alpha-particles, MHD instabilities

* Author to whom any correspondence should be addressed.

^aSee the author list of 'Overview of JET results for optimising ITER operation' by J. Mailloux *et al* to be published in Nuclear Fusion Special issue: Overview and Summary Papers from the 28th Fusion Energy Conference (Nice, France, 10–15 May 2021) for JET Contributors.



Original content from this work may be used under the terms of the [Creative Commons Attribution 4.0 licence](https://creativecommons.org/licenses/by/4.0/). Any further distribution of this work must maintain attribution to the author(s) and the title of the work, journal citation and DOI.

(Some figures may appear in colour only in the online journal)

In a thermonuclear magnetic fusion reactor, the reaction between deuterium (D) and tritium (T) ions, resulting in a fast alpha-particle (^4He) and a neutron, will be the main source of energy: $\text{D} + \text{T} \rightarrow \alpha$ (3.5 MeV) + n (14.1 MeV). In future large-scale fusion devices, such as ITER, fusion-born alpha-particles will provide the dominant source of plasma heating and largely govern the plasma performance [1, 2]. The physics of alpha particle heating is highly non-linear and its extrapolation to future devices is not straightforward. This is partly due to fast-ion driven Alfvén instabilities that alphas can excite over a broad range of frequencies. In turn, the excited modes may cause enhanced radial transport and losses of alpha particles, thereby degrading the plasma confinement and fusion power output [3–5]. Furthermore, ITER can only tolerate fast particle losses of a few percent. Thus, it is crucial to have a solid understanding of AE modes that can be excited by alpha particles. Alfvénic instabilities are usually driven by the free energy from the spatial gradient of the fast-ion distribution function ($\delta\gamma \sim -n\partial f/\partial r$, where n is the toroidal mode number and r the radial coordinate) [6, 7]. Since peaked pressure profiles are expected for alpha particles in burning D–T plasmas, only modes in the ion-diamagnetic direction, i.e. modes with $n > 0$, are currently considered for ITER [5].

In fact, a rich variety of other phenomena is associated with the presence of alpha particles. One of the most important consequences of their presence in ITER are very long sawtooth cycles and monster sawtooth crashes [8–10]. These crashes lead to a periodic reorganization of the plasma core, together with an abrupt drop of the central electron temperature and redistribution of energetic ions.

Present-day discussions on energetic ions in ITER do not usually address synergistic effects triggered by the simultaneous occurrence of various fast-ion phenomena [5]. This paper reports on sawtooth-induced AEs with toroidal mode numbers $n < 0$ (i.e. opposite to the ion-diamagnetic direction) and $n = 0$ (i.e. an axisymmetric mode), which were unexpectedly observed in recent experiments in D- ^3He plasmas with fusion-born alpha particles on the world-largest magnetic confinement fusion device, the tokamak JET (major radius $R_0 \approx 3.0$ m, minor radius $a \approx 0.9$ m). None of these observed modes are currently under consideration for ITER.

1. Experimental results

Dedicated fast-ion experiments in mixed D- ^3He plasmas with $n(^3\text{He})/n_e \approx 20\%–25\%$ were recently performed on JET [11]. In these studies, deuterium ions from neutral beam injection (NBI) with characteristic pitch, $\lambda = v_{\parallel}/v \approx +0.62$ (v_{\parallel} is the ion velocity along the confining magnetic field B) and $E_{\text{NBI}} \approx 100$ keV were accelerated to high energies with waves in the ion cyclotron range of frequencies (ICRF), using the three-ion

D-(D_{NBI})- ^3He scenario [12–14]. Co-passing NBI-injected fast ions with $v_{\parallel} > 0$ reached energies up to ~ 2 MeV, as confirmed by several fast-ion diagnostics, including gamma-ray and neutron measurements. As a result, a relatively high D–D neutron rate $\sim 1 \times 10^{16} \text{ s}^{-1}$ was reached in those D- ^3He L-mode plasmas at moderate input heating power. Simultaneously with the enhanced neutron production, the population of energetic deuterons gave rise to fusion-born alpha particles, originating from the aneutronic reaction $\text{D} + ^3\text{He} \rightarrow \alpha$ (3.6 MeV) + p (14.7 MeV). The production rate of D- ^3He alpha particles was $\sim 2 \times 10^{16} \text{ s}^{-1}$ (based on interpretive TRANSP modeling [15]), which is about twice as large as the D–D neutron rate. The toroidal magnetic field on the magnetic axis $B_0 = 3.7$ T, plasma current $I_p = 2.5$ MA (I_p and B are oriented in the same direction in JET), ICRF settings (RF frequency 32.2–33.0 MHz, dipole antenna phasing), the ^3He concentration, and the central electron density $n_{e0} \approx 6 \times 10^{19} \text{ m}^{-3}$ were chosen for efficient generation and good confinement of energetic deuterons and alpha particles in the JET plasma core.

Figure 1(a) shows an overview of JET pulse #95679 ($P_{\text{NBI}} \approx 6.9$ MW, $P_{\text{RF}} \approx 5.8$ MW, $n(^3\text{He})/n_e \approx 22\%$). ICRF generates a centrally peaked large population of energetic deuterons that results in a strong increase of the central electron temperature and in the D–D neutron rate, raising from $T_{e0} \approx 3.6$ keV and $\sim 5 \times 10^{14} \text{ s}^{-1}$ during the NBI-only phase to $T_{e0} \approx 7.6$ keV and $\sim 1 \times 10^{16} \text{ s}^{-1}$ in the combined ICRF + NBI phase. During this phase, fusion-born alpha particles were produced at a rate $\sim 2 \times 10^{16} \text{ s}^{-1}$, as follows from TRANSP. This corresponds to ~ 60 kW D- ^3He fusion power, which is four times larger than the maximum D- ^3He fusion power (~ 15 kW) reached in JET-ILW ICRF + NBI experiments with 3rd harmonic ICRF heating of D-NBI ions [16]. The sawtooth dynamics in this pulse was rather complex and the duration of the sawtooth-free phases Δt_{saw} varied between 210 ms and 730 ms. A rich family of Alfvén eigenmodes (AEs) was destabilized by fast ions, including the toroidicity- (TAEs, $f \approx 200–260$ kHz) and the ellipticity-induced modes (EAEs, $f \approx 540–600$ kHz), as well as the reversed-shear Alfvén eigenmodes (RSAEs) during the long-period sawtooth-free phases (see figure 4(b) in [11]). Note that the injected fast NBI ions were sub-Alfvénic ($v_{\text{NBI}}/v_A \approx 0.4$; $v_{\parallel, \text{NBI}}/v_A \approx 0.25$) and no AEs were destabilized in the NBI-only phase of #95679.

In this paper, we consider specifically Alfvén instabilities in the EAE frequency range and focus on the modes observed after the monster sawtooth crash at $t \approx 11.035$ s ($\Delta t_{\text{saw}} = 730$ ms). Figure 1(b) illustrates the destabilization of modes in the ion-diamagnetic direction ($n > 0$, starting from $t \approx 11.08$ s), typical for plasmas with a radially peaked population of fast ions such as the ICRF-accelerated deuterons in this experiment. Similar to earlier experiments with ICRF on JT-60U [17], EAEs are located at the $q = 1$ surface (q is

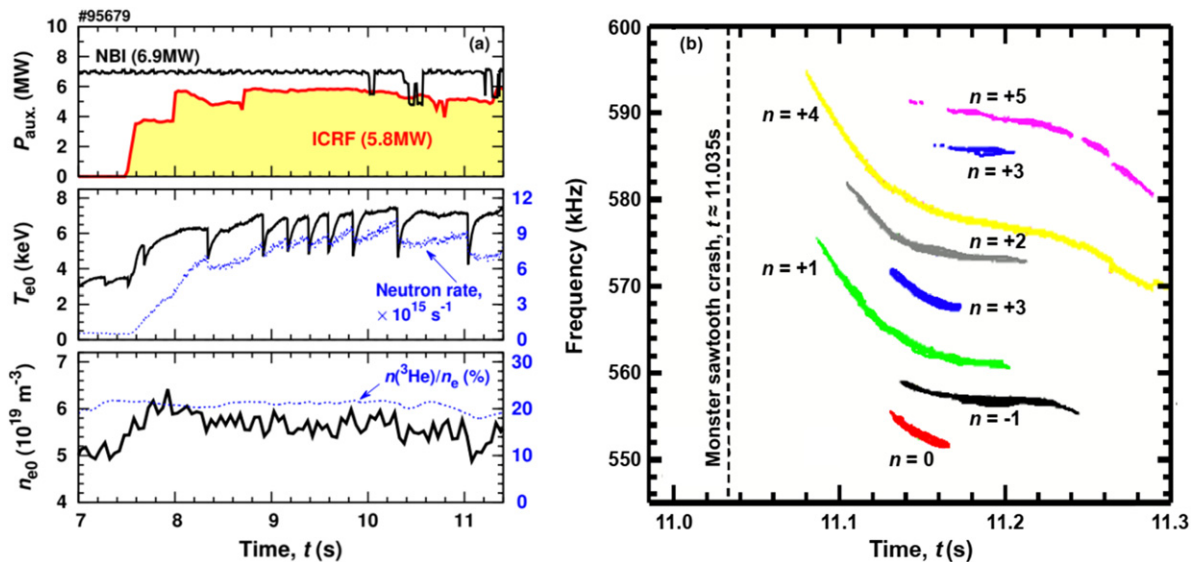


Figure 1. (a) Overview of JET pulse #95679 (3.7 T/2.5 MA) in D-³He plasmas with energetic D-ions and fusion-born alpha particles. (b) Dynamics of Alfvén activities in the EAE frequency range after the monster sawtooth crash at $t \approx 11.035$ s.

the magnetic safety factor). This was inferred from correlation reflectometer measurements (providing the radial mode localization, $R \lesssim 3.25$ m) and sawtooth inversion radius (R_{inv}) analysis. In this pulse, we find that R_{inv} varied between 3.16 m and 3.25 m, when Δt_{saw} increased from 250 ms to 730 ms. Thus, shortly after a sawtooth crash favorable conditions for the destabilization of EAEs with $n > 0$ are present: the $q = 1$ surface is located close to the plasma core, where centrally peaked population of energetic D ions is generated by ICRF. The q -profile evolves during the sawtooth cycle, impacting the evolution of different types of AEs: in particular, the disappearance of EAEs nearly coincides with the appearance of RSAEs. Note that the efficient destabilization of EAEs in this series of fast-ion experiments in D-³He plasmas was also due to the high magnetic field chosen for this experiment ($B_0 = 3.7$ T). Indeed, under these conditions the parallel velocity of the injected fast NBI ions was smaller than $v_A/2$, thereby leading to a negligible EAE damping.

Surprisingly, simultaneously with $n > 0$ EAEs, the $n = -1$ EAE was observed starting at $t \approx 11.14$ s (see figure 1(b)). This was unexpected as the radial-gradient mechanism associated with a radially peaked fast-D population can effectively destabilize modes with $n > 0$, but provides damping for modes with $n < 0$. Furthermore, the global AE (GAE) with $n = 0$ was also destabilized after the monster sawtooth crash. As neither of these two modes are currently considered for ITER, it is important to gain insight in the physics behind these JET observations.

2. Sawtooth-induced redistribution of fast ions

The redistribution of fast ions during the sawtooth crash in tokamaks is complex. Present-day insights indicate that the fast-ion redistribution is pitch-angle or energy dependent, or both, e.g. [18–20]. Yet a widely accepted theoretical model

that is consistent with all experimental observations is so far eluding [21].

Energetic D-ions give birth to both D–D neutrons and D-³He alpha particles. A significant sawtooth-induced redistribution of both energetic deuterons and alphas was observed. The dynamics of fast deuterons during the sawtooth crash was monitored by the neutron camera at JET, which has a temporal resolution of ~ 10 ms. This diagnostic has 19 lines-of-sight, allowing to reconstruct the 2D spatial profile of the neutrons and thus energetic D-ions. Figures 2(a)–(c) show the reconstructed neutron emission profile shortly before and after the monster crash at $t \approx 11.035$ s, illustrating the substantial redistribution of fast-D ions. Figure 2(d) further corroborates this observation: a reduced neutron emissivity in the central channel #5 of the neutron camera and an increased emissivity in channel #6 further off-axis after the crash. By the time the $n = -1$ EAE mode is destabilized, energetic deuterons recover their spatially peaked distribution (cf figure 2(c)) and their radial gradient provides damping for the $n = -1$ mode.

The presence of high-energy alpha particles was independently confirmed by the gamma-ray and fast-ion loss detector (FIELD) measurements. The tomographic reconstruction of the 17 MeV gamma-ray emission (from a weak secondary channel of the D-³He fusion reaction [11, 22]) shows that alpha particles were also localized in the central region of the plasma (see figure 5 in [23]), where EAEs were generated. However, this diagnostic has insufficient temporal resolution to follow the details of the alpha dynamics during the sawtooth crash. In contrast, the FIELD system at JET provides fast signals ($\Delta t \approx 0.5 \mu\text{s}$) of energetic ions escaping the plasma [24]. Figure 3(a) shows a snapshot of lost energetic ions with a Larmor radius $\rho_L \geq 10$ cm ($E_\alpha \geq 4.0$ MeV) and a pitch-angle in the range $\sim 55^\circ$ – 60° shortly after the sawtooth crash ($t = 11.042$ s). The reconstructed orbits shown in figure 3(b) correspond to lost alphas originating from the plasma core. As

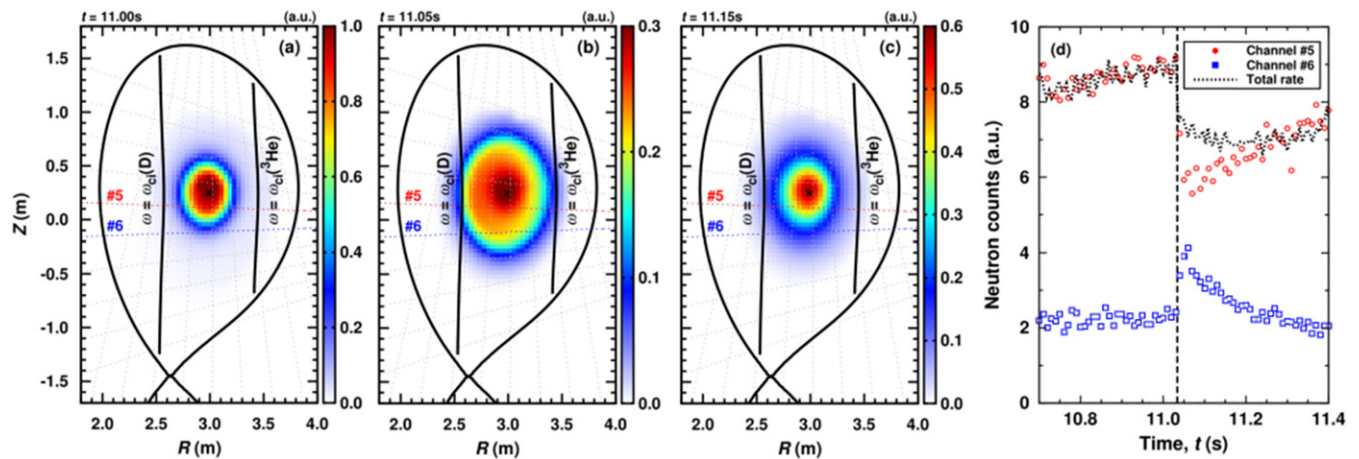


Figure 2. (a)–(c) The reconstructed neutron emission profile in JET pulse #95679 shortly before and after the monster crash at $t \approx 11.035$ s. The dotted lines indicate the lines-of-sight of the neutron camera at JET. (d) Time evolution of the neutron counts during the sawtooth crash, as measured by the channels #5 and #6 of the neutron camera.

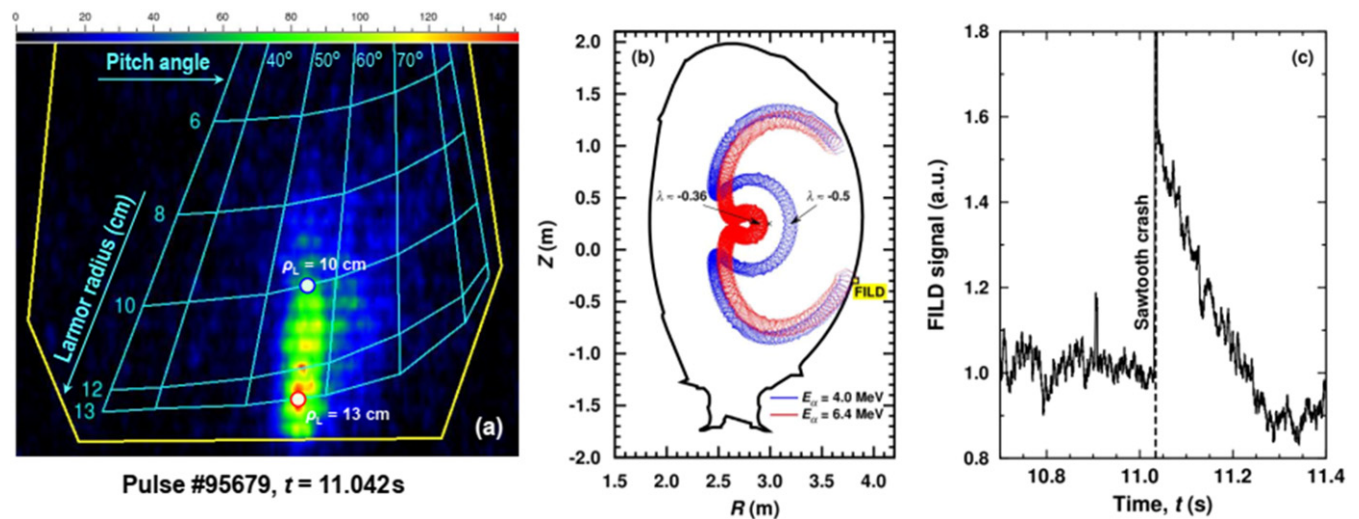


Figure 3. (a) A snapshot of lost energetic ions with Larmor radius $\rho_L = 10$ – 13 cm ($E_\alpha = 4.0$ – 6.4 MeV) and pitch-angle in the range $\sim 55^\circ$ – 60° , measured by FILD shortly after the sawtooth crash ($t = 11.042$ s). (b) The reconstructed orbits of energetic alphas detected by FILD. (c) Time evolution of the lost alpha-particle FILD signal ($\rho_L \geq 11$ cm, $E_\alpha \geq 4.8$ MeV).

shown in figure 3(c), after the sawtooth crash the loss rate of alpha-particles is increased by $\sim 60\%$ with a relaxation time of ~ 200 ms.

Note that alphas are not only redistributed by the sawtooth crash, but also their birth profile is affected by the sawtooth-modified distribution of D-ions. Together with the different dependence of the D–D and D– ^3He reaction cross-sections on the energy of fast deuterons [25], this can lead to alpha distributions with rather non-standard features.

3. Alpha particles and the $n = -1$ mode

Figures 4(a) and (b) show the computed absolute values of the strength of various resonances for the observed $n = -1$ EAE at $f \approx 555$ kHz, assuming fast D-ions and alpha particles as driver of the mode. The plotted quantity is the standard deviation of the particle energy, interacting with the EAE with typical fixed mode amplitude $\delta B/B = 1 \times 10^{-5}$ over 400 wave

periods, as computed with the HAGIS code [26]. A uniform pitch-distribution of test particles (from $\lambda = -1$ to $\lambda = +1$) was used. As expected, the wave-particle interaction occurs along the resonance lines $\omega = n\omega_\varphi - p\omega_\theta$, where ω and n are the AE frequency and the toroidal mode number; ω_φ and ω_θ are the toroidal and poloidal orbital frequencies; p is an integer [7].

The spatial structure of the $n = -1$ EAE was computed by the MISHKA code [27] and is shown in figure 4(c). The relevant EAE gap is produced at the crossing between the poloidal mode numbers $m = 0$ and $m = 2$. The error bars are mainly determined by uncertainties in the safety factor in the central region of the plasma. A monotonic q -profile with a variable value of q_0 was considered in this calculation. With $q_0 \approx 0.95$, both the computed mode frequency and mode localization matched well with the measurements. Figure 4(c) also shows the reconstructed FILD orbits, clearly illustrating the

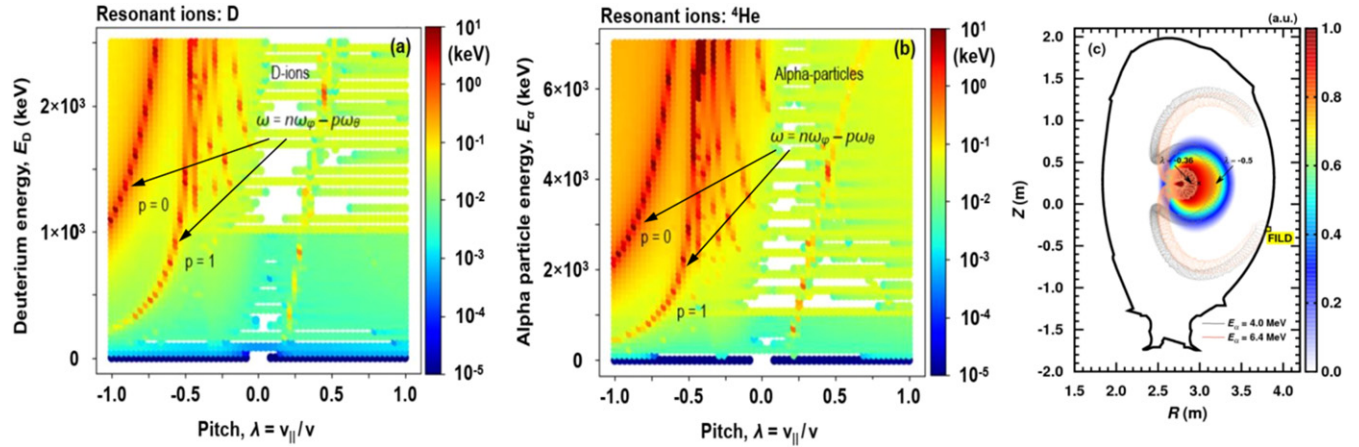


Figure 4. (a) and (b) The computed strength of the resonant wave-particle interaction for the $n = -1$ EAE at $f = 555$ kHz for D ions and alpha-particles. The plotted quantity is the standard deviation of the particle energy (in keV) interacting with the EAE of the amplitude $\delta B/B = 1 \times 10^{-5}$ over 400 wave periods. (c) The computed mode structure (electrostatic potential) of the $n = -1$ EAE together with the reconstructed orbits of lost alphas detected by FILD (see figure 3(b)).

significant overlap between the $n = -1$ EAE mode structure and the region where alpha particles are generated in the plasma.

The resonance maps displayed in figures 4(a) and (b) allow to identify the characteristics of fast ions that resonantly exchange energy with the mode, but they do not distinguish resonances contributing to the mode drive and mode damping. The sign of the resulting energy exchange depends on the details of the fast-ion distribution and the integrals over the distribution function gradients along the resonance lines. As discussed above, the centrally peaked fast-D population provides damping for $n < 0$ modes. Furthermore, as follows from figure 4(a), the resonant exchange of energy for the mode is only possible for energetic deuterons with $\lambda_{\parallel} < 0$, which are virtually absent in this fast-ion experiment, where ICRF accelerates co-passing NBI-injected ions. These two arguments imply that the generated fast deuterons are inefficient to destabilize the $n = -1$ EAE.

In contrast, the distribution function of alpha particles naturally spans the full range of pitch values, thus fulfilling a *necessary* condition for the destabilization of the $n = -1$ EAE (figure 4(b)). Yet the presence of such ions alone is *not sufficient* for the existence of modes with negative toroidal mode numbers. Having a self-consistent modeling of the mode growth rate would be ideal, but it requires a detailed knowledge of the alpha distribution function $f_{\alpha} = f_{\alpha}(E, \lambda, r)$ and its modification during the sawtooth crash, which is particularly complex in these JET experiments. In the absence of a realistic alpha distribution when the $n = -1$ EAE was observed, we cannot provide credible simulations of the mode stability. Instead, in what follows we present conjectures for the origin of the modes, consistent with experimental observations.

Note that non-standard distributions of energetic alpha particles induced by sawtooth crashes were earlier reported in NBI-only D–T experiments on the tokamak TFTR. As discussed in [28], sawtooth crashes resulted in a large drop in the core alpha density and the appearance of radially

hollow alpha profiles (note that $n < 0$ AEs were not reported in [24]). A similar depletion of alphas in the plasma core could also play a role in these JET experiments, as hinted at by the reconstructed FILD orbits (figure 3(b)). Indeed, the orbit-modelling shows that the detected alphas have energies $E_{\alpha} > 4.0$ MeV and pitch between $\lambda \approx -0.5$ and $\lambda \approx -0.36$ in the plasma core, thereby fulfilling a necessary resonance condition for the $n = -1$ mode, shown in figure 4(b). Alphas with lower energies that resonate with the $n = -1$ EAE are also redistributed during the sawtooth crash. However, as these particles have smaller orbits, they do not reach the FILD detector.

Anisotropy of the pitch-angle distribution of fast ions is another source of free energy that can potentially destabilize modes with $n < 0$ [29]. The fast-ion anisotropy term, contributing to the energy transfer, can be expressed as $\delta\gamma \propto (1 - \lambda^2)/(2\lambda E)\partial f/\partial\lambda$. Thus, this mechanism can contribute to the mode drive by energetic ions with $\lambda < 0$, if their distribution fulfills the condition $\partial f/\partial\lambda < 0$. Note the anisotropy drive was reported to be significant only when the mode frequency is close to one of the critical frequencies, ω_{nl} (see the definitions in [30]). The computed frequencies ω_{nl} ($l = 1-3$) are significantly below the experimentally measured $n = -1$ EAE frequency.

A population of fast ions with the inverted energy distribution $\partial f/\partial E > 0$, often referred to as a bump-on-tail, can also contribute to the destabilization of Alfvénic instabilities. This mechanism cannot be at work for the steady-state slowing-down distribution of alphas as it decreases monotonically with energy. Generating a bump-on-tail and thereby impacting the AE stability is possible by modulating the fast-ion source on a time scale shorter than the characteristic fast-ion slowing-down time. This has been successfully demonstrated in recent DIII-D experiments using NBI modulation [31]. In the JET experiments reported here the sawtooth-induced redistribution of fast D-ions provides an intrinsic mechanism for the modification and modulation of the D-³He fusion source of alphas.

The importance of this novel mechanism has not yet been assessed for ITER.

Another unexpected interesting observation is the destabilization of the $n = 0$ GAE in the EAE frequency range at $t \approx 11.13$ s, cf figure 1(b). This mode consists of two dominant poloidal harmonics ($m = \pm 1$) and is also localized in the central region of the plasma. For $n = 0$ modes, the spatial fast-ion gradient does not contribute to the mode drive/damping. Thus, either the anisotropy of the distribution function with respect to the pitch angle [31] or the presence of a positive energy gradient [32], or a combination of both drives these modes unstable. Further detailed mode drive analysis requires a realistic alpha distribution produced by the sawtooth crash. Note that both $n = -1$ and $n = 0$ modes were observed in other pulses of this series of experiments, as well as in previous JET experiments with 3rd harmonic ICRF heating of D ions in D-³He plasmas [33].

4. Importance for ITER and burning D–T plasmas

The reported JET experiments in D-³He plasmas with energetic deuterons and alpha particles clearly demonstrate the non-linear interplay between fast-ion plasma heating, sawtooth stabilization and crashes, and fast-ion-driven AEs. Such synergies will become increasingly more important in ITER and future burning plasma experiments with a large population of fusion-born alpha particles. While the stability of AE modes has been quite extensively analyzed late in the sawtooth cycle [5], a detailed analysis of AEs shortly after the crash has received much less attention. These JET results show that non-standard fast-ion distributions can be generated during the sawtooth crash, in turn, leading to the destabilization of AE modes that are currently not considered for ITER. As AE instabilities are potentially detrimental for the performance and stable operation of ITER, the mere observation of these unexpected modes on JET is an important message for the plasma physics community. We also note a close link between the sawtooth period and the intensity of EAEs in these JET experiments. In particular, EAEs were prominently present in JET pulses with short-period sawteeth.

Our results highlight the need for dedicated modelling activities to further improve knowledge on the complex interplay between the sawtooth-induced redistribution of fast ions and AEs in fusion plasmas. The paper also underlines the particular merit of D-³He plasmas for fusion research, allowing a better understanding of several important aspects for burning reactor plasmas, prior and complementary to future full-scale D–T experiments.

Acknowledgments

This work has been carried out within the framework of the EUROfusion Consortium and has received funding from the Euratom research and training programme 2014–2018 and 2019–2020 under Grant agreement No. 633053 and from the RCUK Energy Programme (Grant No. EP/T012250/1). To

obtain further information on the data and models underlying this paper please contact PublicationsManager@ukaea.uk. The views and opinions expressed herein do not necessarily reflect those of the European Commission.

ORCID iDs

V.G. Kiptily  <https://orcid.org/0000-0002-6191-7280>
 Ye.O. Kazakov  <https://orcid.org/0000-0001-6316-5441>
 J. Ongena  <https://orcid.org/0000-0001-7456-4739>
 M. Nocente  <https://orcid.org/0000-0003-0170-5275>
 S.E. Sharapov  <https://orcid.org/0000-0001-7006-4876>
 M. Dreval  <https://orcid.org/0000-0003-0482-0981>
 J. Garcia  <https://orcid.org/0000-0003-0900-5564>

References

- [1] ITER Physics Basis Expert Group on Energetic Particles 1999 Heating and current drive, ITER physics basis editors. Chapter 5: physics of energetic ions *Nucl. Fusion* **39** 2471
- [2] Fasoli A. et al 2007 Progress in the ITER physics basis. Chapter 5: physics of energetic ions *Nucl. Fusion* **47** S264
- [3] Breizman B.N. and Sharapov S.E. 2011 *Plasma Phys. Control. Fusion* **53** 054001
- [4] Sharapov S.E. et al 2013 *Nucl. Fusion* **53** 103022
- [5] Pinches S.D., Chapman I.T., Lauber P.W., Oliver H.J.C., Sharapov S.E., Shinohara K. and Tani K. 2015 *Phys. Plasmas* **22** 021807
- [6] Wong K.-L. 1999 *Plasma Phys. Control. Fusion* **41** R1
- [7] Heidbrink W.W. 2008 *Phys. Plasmas* **15** 055501
- [8] Porcelli F., Boucher D. and Rosenbluth M.N. 1996 *Plasma Phys. Control. Fusion* **38** 2163
- [9] Budny R.V., Andre R., Bateman G., Halpern F., Kessel C.E., Kritiz A. and McCune D. 2008 *Nucl. Fusion* **48** 075005
- [10] Onjun T. and Pianroj Y. 2009 *Nucl. Fusion* **49** 075003
- [11] Nocente M. et al (JET Contributors) 2020 *Nucl. Fusion* **60** 124006
- [12] Kazakov Ye.O. et al 2017 *Nat. Phys.* **13** 973
- [13] Ongena J. et al 2017 *EPJ Web Conf.* **157** 02006
- [14] Kazakov Ye.O. et al 2021 *Phys. Plasmas* **28** 020501
- [15] Štancar Ž. et al 2021 Experimental validation of an integrated modelling approach to neutron emission studies at JET *Nucl. Fusion* (submitted)
- [16] Sharapov S.E. et al 2016 *Nucl. Fusion* **56** 112021
- [17] Kramer G.J., Cheng C.Z., Kusama Y., Nazikian R., Takeji S. and Tobita K. 2001 *Nucl. Fusion* **41** 1135
- [18] Nielsen S.K. et al 2010 *Plasma Phys. Control. Fusion* **52** 092001
- [19] Salewski M. et al 2016 *Nucl. Fusion* **56** 106024
- [20] Weiland M., Geiger B., Jacobsen A. S., Reich M., Salewski M. and Odstrčil T. (the ASDEX Upgrade Team) 2016 *Plasma Phys. Control. Fusion* **58** 025012
- [21] Jardin S.C., Krebs I. and Ferraro N. 2020 *Phys. Plasmas* **27** 032509
- [22] Kiptily V.G., Cecil F.E. and Medley S.S. 2006 *Plasma Phys. Control. Fusion* **48** R59
- [23] Panontin E. et al 2021 *Rev. Sci. Instrum.* **92** 053529
- [24] Kiptily V.G. et al 2018 *Nucl. Fusion* **58** 014003
- [25] Bosch H.-S. and Hale G.M. 1992 *Nucl. Fusion* **32** 611
- [26] Pinches S.D. et al 1998 *Comput. Phys. Commun.* **111** 133
- [27] Mikhailovskii A.B. and Sharapov S.E. 1997 *Plasma Phys. Rep.* **23** 844

- [28] Stratton B.C., Ponck R.J., McKee G.R., Budny R.V., Chang Z., Wising F. and Ödholm A. 1996 *Nucl. Fusion* **36** 1586
- [29] Vernon Wong H. and Berk H.L. 1999 *Phys. Lett. A* **251** 126
- [30] Van Zeeland M.A. *et al* 2021 *Nucl. Fusion* **61** 066028
- [31] Fu G.Y. 2008 *Phys. Rev. Lett.* **101** 185002
- [32] Berk H.L., Breizman B.N. and Ye H. 1992 *Phys. Rev. Lett.* **68** 3563
- [33] Oliver H.J.C., Sharapov S.E., Breizman B.N. and Zheng L.-J. (JET Contributors) 2017 *Phys. Plasmas* **24** 122505